A LTE MIMO OTA Test System Using Vector Signal Transceivers

Chong Li, Tian-Hong Loh, David A. Humphreys,
Time, Quantum and Electromagnetics Division
National Physical Laboratory, Teddington, Middlesex, UK
chong.li@npl.co.uk; tian.loh@npl.co.uk; david.humphreys@npl.co.uk
Yunsong Gui, Haowen Wang
Shanghai Research Centre for Wireless Communications, Shanghai, China
Fei Qin
Key Laboratory of Wireless Sensor Network & Communication, Shanghai Institute of Microsystem and Information Technology, Chinese Academy of Sciences, Shanghai, China

***Abstract*—A 2 × 2 multiple-input-multiple-output over-the-air (MIMO OTA) test system based on four field-programmable Vector-Signal-Transceiver (VST) modules is presented. The system enables 2 x 2 MIMO OTA testing by assembling of a two-channel Evolved Node B (eNodeB) LTE base station emulator, a 2x2 channel emulator, and a two-channel user equipment (UE) simulator. A two-stage MIMO OTA test method has been demonstrated with downlink Long-Term Evolution Time-Division Duplex (LTE-TDD) mode using different modulation and coding schemes (MCSs). Test results and analysis are shown. This system will allow a systematic study of MIMO OTA metrology needs.**

Keywords— LTE TDD, MIMO OTA measurement, FPGA, SDR.

I. Introduction and Motivation

Wireless communications, as a world-wide business, is dependent on specification standards for manufacture, harmonization and interoperability. Industry standards organizations such as 3GPP (Third Generation Partnership Project), ETSI (European Telecommunications Standards Institute) and CTIA (International Association for the Wireless Telecommunication Industry) are in turn underpinned by mathematical algorithms and physical measurement, traceable to national measurement institutes such as NPL (National Physical Laboratory) in the United Kingdom, and NIST (National Institute of Standards and Technology) in United State of America.

There is continuous pressure to improve the capacity of mobile communication systems. The currently deployed fourth-generation (4G) long-term evolution (LTE) technology systems use additional antennas and multiple-input-multiple-output (MIMO) algorithms to increase channel capacity and overcome fast-fading caused by multi-path propagation in the environment. Increasing the number of MIMO antennas also improves spatial diversity and allows frequency re-use.

C. Li, T.-H. Loh and D. A. Humphreys were supported by the European Metrology Research Program (EMRP) through the IND51 Joint Research Projects, *Metrology for Optical and RF Communications Systems* (MORSE), and by the 2014 – 2016 Electromagnetic Metrology Program of the National Measurement Office, an Executive Agency of the U.K. Department for Business, Innovation and Skills. The EMRP was supported by the EMRP participating countries within EURAMET and the European Union. Y. Gui and H. Wang were supported by the National Science and Technology Major Project of China under Grant Project 2014ZX03003012-001. F. Qin was supported by the Open Project Scheme, Grant No. 2013004, from the Key Laboratory of Wireless Sensor Network & Communication, Chinese Academy of Sciences.

II. Definition of the Problem

Reliable measurement of a MIMO system (often being refer to as user equipment (UE)) over-the-air (OTA) is a key problem. Several MIMO OTA test-methods [1], [2] have been adopted within standards [3], [4] but continued research activities [5], [6] indicate that the measurement issues have not been fully resolved.

To provide a level playing-field, channel emulation models such as Jakes [7], [8] and Spatial Channel Model Extended (SCME) [9], [10] models, can be used to mimic the multipath contribution from the environment. Fig. 1 illustrates the problems with conducted and radiated test for the MIMO OTA two-stage method. The simplest MIMO OTA testing approach is two-stage conducted test where antenna radiation pattern is measured in stage one and in stage two the radio frequency (RF) signals from the channel emulator (CE) are bypassing the antennas and directly injected at the MIMO system receiver ports. This verifies the RF hardware and the ability of the UE signal processing to solve the MIMO matrix inverse problem under defined noise conditions. While this technique is attractive

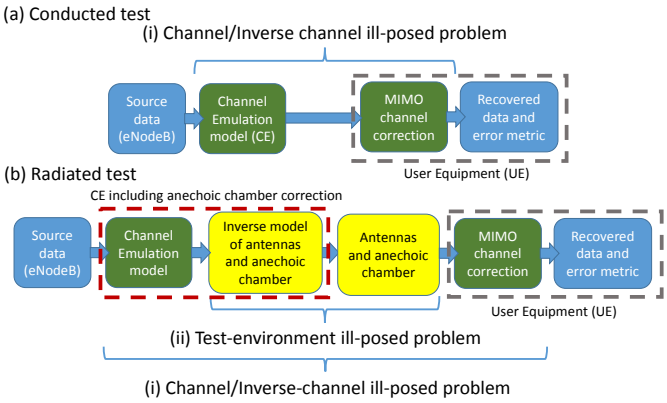

Fig. 1. Illustration of problems with conducted and radiated test for the MIMO OTA two-stage method.

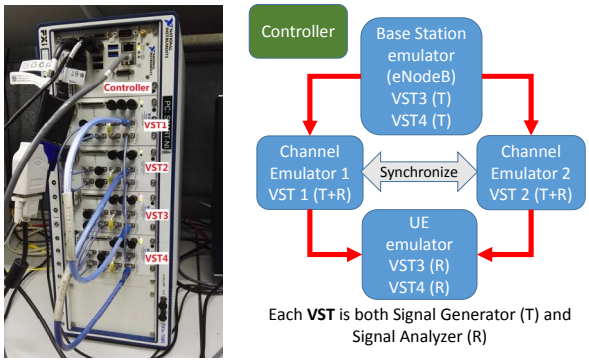

(a)

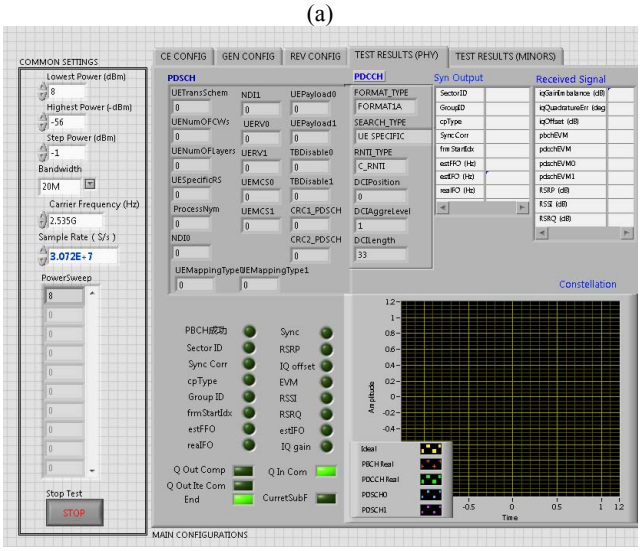

(b)

Fig. 2 Illustration of the 2 × 2 MIMO OTA measurement system using four VST modules (a) and its graphic user interface (b).

during the development phase of the MIMO system, by allowing the ability to measure the MIMO system performance with various antenna configuration, it assumes that there is minimal interaction between internal spurious emissions from MIMO system radio hardware and the MIMO antenna array.

As depicted in Fig. 1, when the measurement is carried out over the air the antenna contributions will modify the result and may make the problem ill-conditioned. Also, correcting the multi-path environmental contribution is an ill-posed problem as the real world multi-path environment is not stationary. These data are used to construct an inverse matrix that compensates for path loss, delay and polarization between the channels for signals arriving from a certain angle. Depending on the correlation between the antennas in the test environment this inverse matrix may be well-conditioned or ill-conditioned. Hence the problem becomes one of two parts: (i) verify the conducted and radiated test results are identical; (ii) develop traceable OTA radiated test measurement method for determination of different UEs behavior. In this paper, we describe progress of ongoing work at NPL to provide metrological support for the MIMO OTA two-stage test method [1]. The performance of the receiver signal-processing algorithms is determined using measurement of throughput and other metrics such as BLER (Block Error Rate) and constellation diagrams.

III. The MIMO-OTA Test System

The MIMO OTA test system consists of four vector signal transceiver (VST) modules [11] and a controller. The VST is a new class of instrumentation that combines a vector signal generator (VSG) and a vector signal analyzer (VSA) with a field-programmable gate array (FPGA)-based real-time signal processing and control. Each VST has a bandwidth of 80 MHz and operates from 65 MHz to 6 GHz with a maximum continuous wave (CW) power of +15 dBm. Each VST has separate local oscillators (LOs), real-time signal processing and reference clocks for both the transmitter and the receiver hardware to allow independent, simultaneous transmission and reception. In addition, multiple units can be synchronized through the RF connections to form a larger, scalable system. Both receive and transmit functions of a VST are used to provide channel emulation or emulate both LTE signal generation and transmission and receive and analysis. Fig. 2 shows the MIMO-OTA system and its graphic user interface.

As depicted in Fig. 2(b), all parameters for the hardware setup and for the LTE physical downlink channel configuration can be defined from the user graphic interface front panel of the base-station (eNodeB) emulator. The baseband signal processing is performed using a Dynamic-link library (DLL) and the FPGA. The receiver channel estimation is based on a Least-squares (LS) estimation with linear interpolation in both the time and frequency domains.

The CE used here is a modified version of a freely available 2 × 2 CE [8] that includes a Matlab interface and allows antenna parameters, such as radiation pattern, to be used as input parameters. This CE can operate in either stochastic or deterministic modes. The stochastic mode uses modified Jakes model [7] with fading parameters such as time delay and antenna correlations to generate fading channel coefficients. Verification of this CE system was presented in [12]. Antenna correlations can be obtained from radiation pattern of the MIMO antenna, measured in an anechoic chamber. In deterministic mode, the faded channel coefficients are generated directly from the SCME channel model [9] and [10], where channel fading parameters, antenna radiation pattern, angle of arrivals etc. are required.

IV. Experiments

The system provides a downlink function for LTE-TDD based on 3GPP Release 8 [13]. The two-stage MIMO-OTA conducted and radiated tests were performed with and without CE. Three different modulation methods were tested: Quadrature Phase-Shift Keying (QPSK), 16-state and 64-state Quadrature Amplitude Modulation (16-QAM and 64-QAM), corresponding to 2, 4 and 6 bits per symbol respectively. The corresponding modulation and coding schemes (MCS) index for the Physical Downlink Shared Channel (PDSCH) are 1, 16 and 20, respectively referring to Table 7.1.7.1-1 in 3GPP TS 36.213 V8.8.0 (2009-10) [13]. The maximum throughputs for the three MCSs are 1.19 Mbps, 10.05 Mbps, and 12.89 Mbps, respectively. For each modulation scheme we carried out five measurement runs to evaluate the repeatability of the test. The key parameters are summarized in Table I.

TABLE I. PARAMETERS USED WHEN EVALUATING THE SYSTEM

Item	Value	Units
Centre Frequency	2.535	GHz
Bandwidth	20	MHz
Number of Frequency Carriers	1	-
Frame Configuration	0	-
Special Frame Configuration	1	-
User Equipment Transmission mode	2	-
PDSCH MCS	1, 16, 20	-
Transmission Scheme	Transmit Diversity	-

A. Two-stage OTA Test: Conducted

As depicted in Fig. 3, for the measurement setup without CE, the eNodeB emulator (VSTs 3 and 4) and UE simulator (VSTs 1 and 2) are directly connected via two short RF cables, whereas for the measurement setup with CE, VSTs 3 and 4 are used to generate an LTE downlink signal which is fed to the CE (VSTs 1 and 2); the output signal from the CE is fed to the input of VSTs 3 and 4 for analysis. Note that with this setup configuration there is no need to remove the wire between VSTs 3 and 4 outputs and VSTs 1 and 2 inputs but simply modifying the software setup. Fig. 4 shows the accumulated constellation diagrams of individual LTE subframes of arbitrary frames for different MCSs with CE (right column) and without CE (left column). Colors of yellow, pink, red, green, and purple represent ideal and measured QPSK, and measured Physical Broadcast Channel (PBCH), Physical Downlink Control Channel (PDCCH), Physical Downlink Shared Channels (PDSCH 1 and 2), respectively. As expected, the signals for PBCH (QPSK), PDCCH (QPSK), and PDSCH (QPSK when MCS is 1) surround around the ideal QPSK in the constellation points but show

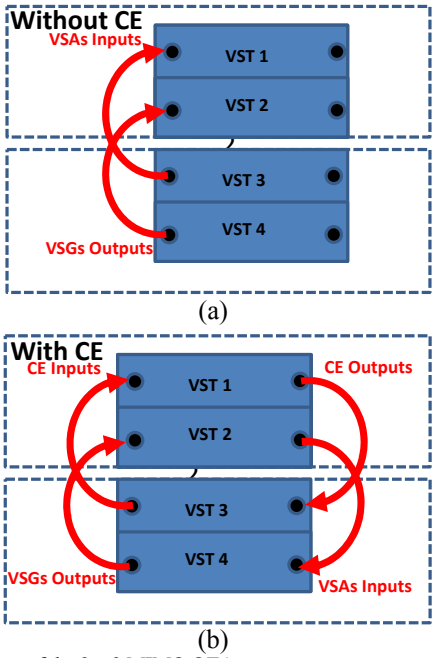

Fig. 3 Illustration of the 2 × 2 MIMO OTA measurement system using four VST modules: (a) without CE; (b) With CE.

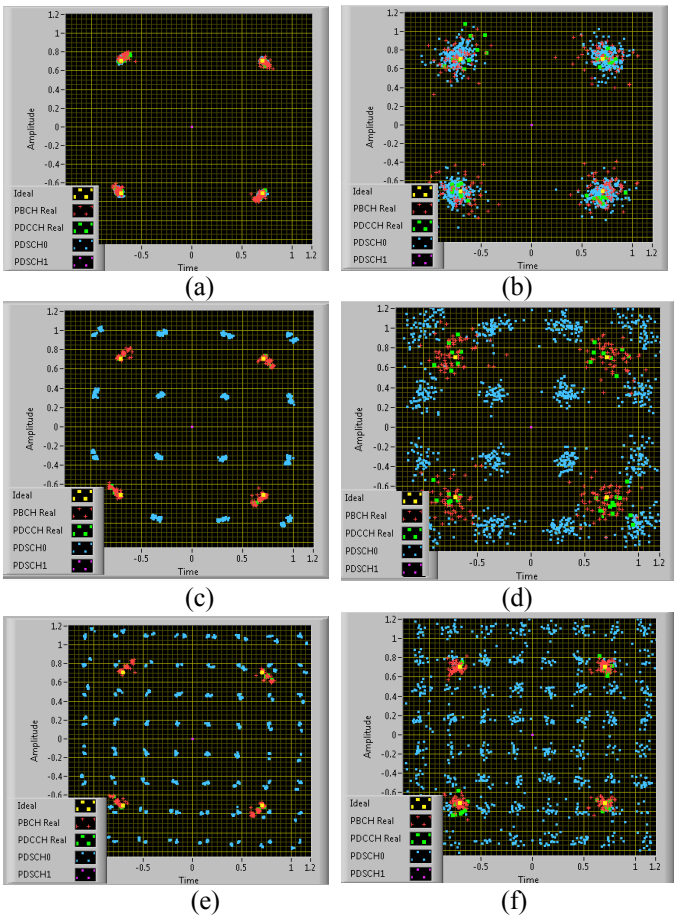

Fig. 4 Captured constellation diagrams of the 2 × 2 MIMO OTA system without (a, c & e) and with (b, d & f) channel emulation for different PDSCH modulation methods QPSK (a & b), 16-QAM (c & d) and 64-QAM (e & f).

increased scatter about the constellation points when the CE is used. Similar behaviors are found in PDSCH with 16 QAM and 64 QAM for MCS 16 and 20, respectively. This masks the phase-noise errors and a residual Inter-Symbol Interference that are present in the uncorrupted measurement.

TABLE II. ANALYSIS OF MODULATION PENALTY COMPARED TO QPSK AT 50% THROUGHPUT WITH UNEXPANDED UNCERTAINTIES ($K = 1$)

Conditions	Modulation	
	16-QAM (dB)	*64-QAM (dB)*
Theoretical	7.0	13.2
Without CE	8.9 ±0.04	12.0 ±0.04
With CE	3.3 ±0.05	6.9 ±0.11

Fig. 5 shows the throughput variation with the indicated total source RF power of the eNodeB emulator both with and without CE for different MCSs, where the source power was swept from high to low as the system throughput varying from 100% to 0%. As expected, the higher-order modulation formats require a higher power level. It is noted that the relationship between the results with and without the CE are indicative and have not been corrected for absolute power calibration or for the mean loss

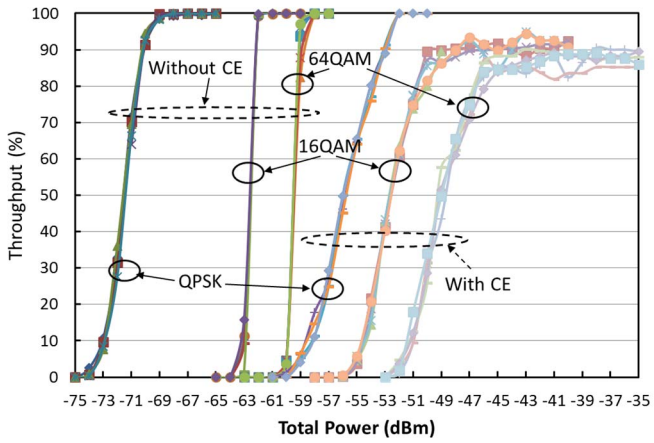

Fig. 5 Throughput measurement of the system with and without CE for Two-stage OTA conducted test with different modulation methods and its repeatability assessment.

within the CE. Table II shows the comparison of the modulation penalty in dB between the theoretical value [14] and the system operating with and without CE for 16-QAM and 64-QAM as compared to QPSK at 50% throughput in which the unexpanded uncertainty is calculated from the measured results. While the directly connected measurement and the theoretical value give similar results with a 1-2 dB difference, it is interesting to note that difference is much reduced when using the CE. Also, 100% throughput cannot be achieved for either 16-QAM or 64-QAM. We believe that this may be due to the non-ideal channel equalization caused by the linearly-interpolated LS-based channel estimation of the receiver, which brings the diffusion of constellation as depicted in Figs. 4(c) - 3(f).

B. Two-stage OTA Test: Radiated

We carried out preliminary radiated OTA test using two cross-polarized 45 degree slant MIMO antennas [15] at a fixed distance of 1.6 m in an anechoic chamber (AC). The setup in the AC is shown in Fig. 6 and the complete setup is illustrated in Fig. 7. Modified Jake's model was used in the CE which has an assumption of a vertical receiver antenna with infinite number of equi-gain and equiangular rays impinging on it [7]. The radiated channel matrix [1] was measured with CW generated by VSTs and the frequency span was 20 MHz and centered at 2.535 GHz. The indicated source RF power was set to be - 15 dBm.

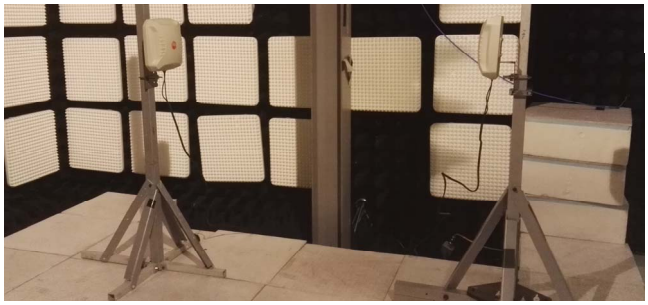

Fig. 6 Radiated test setup in an anechoic chamber.

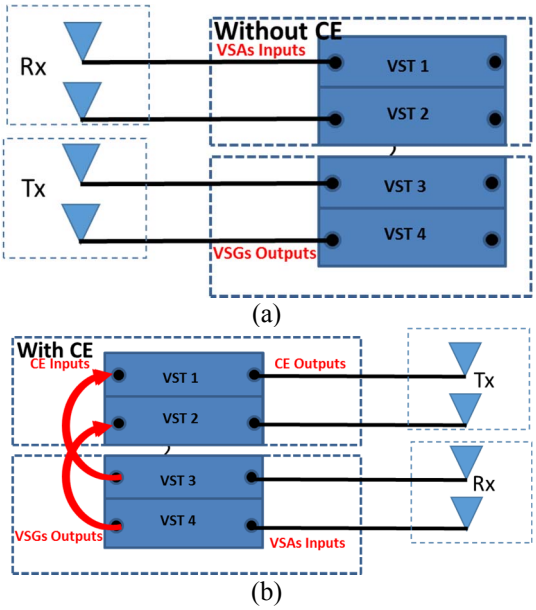

Fig.7. Illustrations of radiated test setups: (a) without CE; and (b) with CE.

As depicted in Fig 8, the measured radiated channel matrix, h = {h(1,1), h(1,2); h(2,1), h(2,2)} shows low correlation with the cross polarization power ratio (XPR) (i.e. (h(2,1)-h(1,1)) and (h(1,2)-h(2,2)) [1] of greater than 15 dB. This result indicates that the corresponding receive and transmit antennas are "properly aligned" and can maximize h(1,1) and h(2,2). It is close to the conducted test where two channels are completely uncorrelated [16]. For the radiated OTA test setup without CE as illustrated in Fig. 7(a), VSTs 3 and 4 were set as an eNodeB emulator to generate downlink LTE signals which were then fed to the transmitting antenna feed ports (left in Fig. 6) and the VSTs 1 and 2 were set to work as UE which was connected to the receiving antenna feed ports (right in Fig. 6). In the case of radiated test with CE as illustrated in Fig. 7(b), the output of VSTs 3 and 4 were directly fed to the input of the CE (VSTs 1 and 2) and the outputs of the CE were fed the transmitting antenna ports and then the receiving antenna feed ports were fed to the inputs of UE (VSTs 3 and 4).

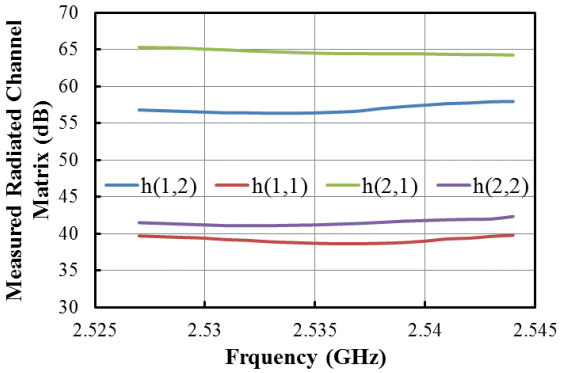

Fig. 8 Measured radiated channel matrix in the radiated test.

Both radiated test results using QPSK with and without CE are plotted in Fig. 9. The results shown in Fig. 9 agree with the results obtained using conducted tests (Fig. 5) once the system loss is taken out. Note that the throughput with CE shown in Fig. 9 starts to decrease above a power level of about 7 dBm. This is because the power level exceeds the maximum limit of

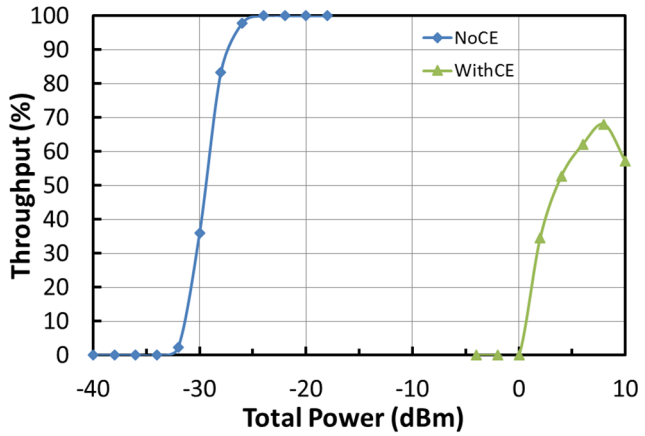

Fig. 9 System throughput with CE and without CE for radiated test using QPSK.

the VSTs. Two methods to avoid this by reducing the required source power level from the eNodeB are to either insert a power amplifier with high linearity between the VSTs and the antenna feed port or else to reduce the separation between the antennas to reduce the propagation loss.

V. Conclusions and Future Work

In this paper, we have outlined the motivation for this work and presented a 2 × 2 MIMO OTA test system implemented using VSTs. The VST system offers a degree of flexibility and can be adapted as new standards and protocols emerge. We have demonstrated the LTE-TDD 'two-stage' tests using different MCSs for both conducted and radiated (OTA) setups with and without CE. The results showed that with the CE present in the system the 16-QAM and 64-QAM modulation formats could not achieve 100% throughput. The exact cause has not yet been unambiguously determined at this point.

The dependence of RF power accuracy for throughput measurements is important. We were able to demonstrate the relative dependence of source RF power on modulation at 50% throughput threshold depends on the modulation format and whether channel emulation has been applied. We expected the relative dependence on MCS without CE would agree with the theoretical values (Table II) but this was not observed. However, indicated source values, rather than RF power measurements were used for the comparison. We will investigate the source of this discrepancy in the future.

Acknowledgment

The authors would like to thank Georgios Tsalavoutis of National Instruments for his help on VST hardware synchronization and thank Moray Rumney and the members of the EMRP MORSE project steering board for their valuable comments.

References

[1] Rumney, R. Pirkl, M.H. Landmann, and D.A. Sanches-Hernandez. "MIMO over-the-air research, development, and testing", Intenational Journal of Antennas and Propagation, Vol. 2012, 2012, pp. 1–8.

[2] Glazunov, V.-M. Kolmonen and T. Laitinen, "MIMO over-the-air testing", Chapter 15 in "LTE-advanced and next generation wireless networks: channel modelling and propagation", Editors: G. Roche, A. A. Glazunov, and Ben Allen, Wiley-Blackwell, Nov. 2012, pp. 411 – 441.

[3] 3GPP TR 37.977 V13.1.0 (2015-09), "Verification of radiated multi-antenna reception performance of User Equipment (UE)", Sep. 2015.

[4] CTIA, V1.0, "Test plan for 2x2 downlink MIMO and transmit diversity over-the-air performance", Aug. 2015.

[5] COST Action 2100 Available: http://www.cost2100.org/.

[6] COST Action IC1004 Available: http://www.ic1004.org/.

[7] Y. Zheng and C. Xiao, "Simulation models with correct statistical properties for Rayleigh fading channels," *IEEE Transactions on Communications*, Vol. 51, No. 6, pp. 920-928, 2003.

[8] Real-time MIMO channel emulation on the NI PXIe-5644R. Available at: http://zone.ni.com/devzone/cda/epd/p/id/6556.

[9] D. S. Baum, J. Salo, G. Del Galdo, M. Milojevic, P. Kyösti, and J. Hansen, "An interim channel model for beyond-3G systems," *in Proc. IEEE VTC'05*, Stockholm, Sweden, May 2005.

[10] 3GPP Spatial Channel Model Extended (SCME), Available at http://projects.celtic-initiative.org/winner+/3gpp_scme.html.

[11] National Instruments PXIe-5644R 6 GHz Vector Signal Transceivers, available: http://sine.ni.com/nips/cds/view/p/lang/en/nid/210629.

[12] T. H. Loh, C. Li, H. Wang, and F. Qin, "A Software-Defined-Radio Platform for Multiple-Input-Multiple-Output Over-The-Air Measurement ," in Proceedings of EUCAP 2016. Davos, Switchland, 10-15 Apr. 2016.

[13] 3GPP Release 8 TS 36.213. "Physical layer procedures." *3rd Generation Partnership Project; Technical Specification Group Radio Access Network; Evolved Universal Terrestrial Radio Access (E-UTRA)*. Available at: http://www.3gpp.org/specifications/releases/72-release-8.

[14] S. Brand, "QAM Demodulation", available at: http://www.wirelesscommunication.nl/pdfandps/qam.pdf.

[15] Poynting model XPOL-A0002. Available at: http://www.solwise.co.uk/4g-antenna-panel-xpol-a0002.html.

[16] M. Rumney, H. Kong, Y. Jing, Z. Zhang, and P. H. Shen, "Recent Advances in the Radiated Two-Stage MIMO OTA Test Method and Its Value for Antenna Design Optimization," in Proceedings of EUCAP 2016. Davos, Switchland, 10-15 Apr. 2016.